

# Effect of butylphthalide intervention on experimental autoimmune myositis in guinea pigs

JUAN CHEN<sup>1,2</sup>, JINGYANG WANG<sup>1</sup>, JIYAN ZHANG<sup>3</sup> and CHUANQIANG PU<sup>1</sup>

<sup>1</sup>Department of Neurology, Chinese PLA Medical School, Beijing 100853; <sup>2</sup>Department of Neurology, The 309th Hospital of PLA, Beijing 100091; <sup>3</sup>Department of Immunology, Academy of Military Medical Sciences, Beijing 100850, P.R. China

Received December 4, 2015; Accepted December 19, 2016

DOI: 10.3892/etm.2017.5416

**Abstract.** Idiopathic inflammatory myopathies are a group of rare muscular diseases that are characterized by acute, subacute or chronic proximal and symmetric muscle weakness, muscle fiber necrosis and infiltration of inflammatory cells, particularly activated CD8<sup>+</sup> cytotoxic T cells and phagocytes. 3-n-butylphthalide (NBP) protects mitochondria and reduces the inflammatory response in multiple disease models. In myositis, it has remained elusive whether NBP can protect muscle cells from muscle fiber injury. Experimental autoimmune myositis (EAM) was induced in a total of 40 guinea pigs by myosin immunization. After 4 weeks, low- or high-dose NBP solution was intraperitoneally injected. Saline solution was used as a negative control. After 10 days, the clinical manifestations were assessed by determining rodent grasping power, histopathological changes, Ca<sup>2+</sup>-adenosinetriphosphatase (ATPase) activity by an ATPase kit, and mRNA expression of interferon (IFN)- $\gamma$ , retinoic acid receptor-related orphan nuclear receptor (ROR) $\gamma$ t and forkhead box (Fox) p3 in muscle tissue by reverse-transcription quantitative polymerase chain reaction analysis. It was demonstrated that NBP improved the myodynamia of guinea pigs with EAM and reduced the pathological inflammatory cell infiltration in a dose-dependent manner. NBP improved the Ca<sup>2+</sup>-ATPase activity of the muscle mitochondrial membrane and muscle plasma membrane in animals with EAM. It also reduced the mRNA expression of IFN- $\gamma$  and ROR $\gamma$ t, and significantly increased the mRNA expression of Foxp3 in muscle tissue. These results provided a basis for the consideration of NBP as a novel agent for the treatment of myositis and other muscular diseases associated with autoimmunity and inflammation.

## Introduction

The clinical manifestations of idiopathic inflammatory myopathies include symmetrical proximal myasthenia, reduced maximum lactate value capacity and muscle inflammation, with general symptoms of fatigue, weakness, depression, weight loss, muscular pain and myophagism (1,2). Pathological manifestations include muscle fiber necrosis and infiltration of inflammatory cells, particularly activated CD8<sup>+</sup> cytotoxic T cells and phagocytes (2-4). In general, patients respond well to standard immunosuppressive therapies, such as glucocorticosteroids and intravenous immunoglobulins (5-7). However, a large number of patients are resistant to current therapies, and treatment of idiopathic inflammatory myopathies still remains a formidable challenge (8).

3-n-Butylphthalide or (NBP) is a chemical ingredient of celery oil (9). Studies have demonstrated that NBP reduces cerebral infarction and neurologic impairment induced by diabetes (10,11). In addition, NBP has been reported to have inhibitory effects on inflammation following focal ischemic brain injury in rats (12). NBP also attenuates the amyloid- $\beta$ -induced inflammatory responses in cultured astrocytes via the nuclear factor- $\kappa$ B signaling pathway (13).

The present study investigated the effect of intervention with NBP on idiopathic inflammatory myopathies. A guinea pig model of experimental autoimmune myopathy (EAM) to mimic idiopathic inflammatory myopathies in humans. It was demonstrated that NBP improves the myodynamia of EAM animals and reduces pathological inflammatory cell infiltration in a dose-dependent manner. The results suggested that NBP should be developed as a novel therapeutic agent for idiopathic inflammatory myopathies.

## Materials and methods

**Animals.** A total of 40 female guinea pigs (British white shorthair Dunkin, Hartley strain; age, 6-8 weeks; weight, 250-300 g) were obtained from the Military Academy of Medical Sciences Laboratory Animal Center (Beijing, China), where they were bred in-house. The quality of the guinea pigs had been tested by the State Food and Drug Administration Academy (Beijing, China) with laboratory animal production license no. SCXK, 2012-0004. The animals were housed in the Fengtai animal house of the Laboratory Animal Center of

---

*Correspondence to:* Dr Chuanqiang Pu, Department of Neurology, Chinese PLA Medical School, 28 Fuxing Road, Beijing 100853, P.R. China  
E-mail: cq30128@sina.cn

**Key words:** experimental autoimmune myopathy, butylphthalide, experimental autoimmune myositis, guinea pigs, muscle pathology, Ca<sup>2+</sup>-ATPase, mRNA expression in muscle tissue

the Military Academy of Medical Sciences (Beijing, China). The environmental conditions including noise and cleanliness complied with national standards, with an indoor temperature of 18-22°C, 45-60% humidity and a 12 h light/dark cycle. Animals were fed guinea pig silage and fresh cabbage. The animal diet was verified prior to experimentation. Immunization was performed after 7 days. Each animal was weighed every week and observed for dietary intake, behavior and mental state. The animal experiment was approved by the People's Liberation Army (PLA) General Hospital and the Military Medical Science Animal Ethics Committee (Beijing, China). All procedures involving laboratory animals were performed according to the National Institutes of Health's Guiding Principles on the Care and Use of Animals.

**Immunization.** Immunization of guinea pigs was performed according to the method of Nemoto *et al.* (11). Purified rabbit myosin (5 mg/0.5 ml; cat. no. M1636), complete Freund's adjuvant (CFA; cat. no. F5881) and pertussis toxin (PT; cat. no. P7208; 50 µg/500 µl) were from Sigma-Aldrich (Merck KGaA; Darmstadt, Germany). *Mycobacterium tuberculosis* toxin (MTT; 600 mg inactivated bacteria, diluted with 5 ml normal saline, subjected to repeated freezing and thawing) was provided by the Tuberculosis Research Center of the 309th Hospital of the Chinese PLA (Beijing, China). To immunize the animals, 0.3 µl purified rabbit myosin (3 µg total; 5 mg/0.5 ml), 0.1 ml CFA and 10 µl MTT (1.2 mg total; 120 mg/ml) (14) were mixed with 0.2 ml normal saline. After thorough oscillation in a vortex mixer, the white emulsion was injected subcutaneously at multiple sites on the backs of guinea pigs. The injection was administered once a week for a total of 4 weeks. For the first 2 immune injections, each guinea pig was injected intraperitoneally with pertussis toxin at 500 ng/200 µl (14).

**NBP treatment.** The EAM guinea pigs were randomly divided into the EAM/normal saline group (n=10), EAM/low-dose NBP group (n=10), and EAM/high-dose NBP group (n=10). NBP (1 g/ml) was provided by the Shiyao Pharmaceutical Co., Ltd. (Shijiazhuang, China). The NBP was dissolved in 0.5% Tween 80 (Beijing Keino Spring Biological Technology, Co., Ltd., Beijing, China) (15) and injected intraperitoneally into the EAM animals in the morning twice a week for 2 weeks at 40 µl/40 mg/kg wt (low dosage) or 80 µl/80 mg/kg wt (high dosage). For the normal saline group, the animals were injected with Tween 80 (5 g/kg wt) and normal saline (10 ml/kg wt).

**Clinical observation.** The investigator was blinded to animal grouping. Rodent grasping power (as an indicator of strength) was determined using a grasping power apparatus (model no. KH-YLS13A; cat. no. 53007; maximum tension, 2,000 g; Beijing Kai Hui Shengda Technology Development Co., Ltd., Beijing, China) (16). The animal forelimbs were connected with a dynamometer, which records the maximum force on a wire grid (17). The range of power production is influenced by factors such as muscle inflammation, connective tissue changes, and spinal cord or brain neural plasticity (18). The tests were performed in triplicate and the tested maximum force (g) was regarded as the holding power.

**Biopsy and sample preparation.** Guinea pigs were anesthetized via intraperitoneal injection of 50 mg/kg sodium pentobarbital (Sigma-Aldrich; Merck KGaA) to prevent excessive struggle (19-26). A thoracotomy was performed and a needle was inserted into the right ventricle to harvest ~10 ml blood for use in the following experiments. Following blood harvest, guinea pigs skeletal muscle specimens were obtained from thigh muscles in the limbs of guinea pigs.

The sheared fresh muscle tissue was dissected (5 mm diameter, 1 cm length), and fixed using tragacanth gum. Approximately 1 l liquid nitrogen was placed into a heat insulation barrel, and a 100 ml beaker with a 30 cm iron wire handle was filled with 70-80 ml isopentane. The beaker was submerged in liquid nitrogen, and a specimen block was added and stirred continuously with large tweezers for 30 sec to freeze the specimen without ice crystals forming. The specimen was placed into liquid nitrogen for 30-60 min, until isopentane around the specimens had vaporized, and subsequently stored in sealed plastic bags at -80°C overnight. Specimens were subsequently heated to -25°C for 30 min and sliced into transverse sections (thickness, 5 µm) using a sharp blade. Slices were stored at -25°C for staining. A portion of the muscle tissue from the distal and proximal limbs of each of the 40 guinea pigs was prepared as a frozen section, with 8 sections per guinea pig. Fresh muscle tissues (50-100 mg) were immediately placed in sterilized cryopreserved tubes, immersed in liquid nitrogen and stored at -80°C for subsequent analysis using polymerase chain reaction.

**Hematoxylin and eosin (HE) staining and histopathological examination.** Samples were stained in Harris hematoxylin solution for 10 min, rinsed in water for 10 min, stained in 1% eosin for 3 min, and then repeatedly rinsed in water. After dehydration in ethanol, the samples were rinsed in xylene and coated with balata. Pathological scores were determined by observing 4 visual fields per section under a light microscope (Olympus-BX43; Olympus Corporation, Tokyo, Japan). Scoring of inflammation was performed using the following classification method (27,28): 1, ≤5 muscle fibers involved; 2, damage involving 5-30 muscle fibers; 3, damage involving 1 muscle bundle; 4, diffuse, extensive damage, involving >1 muscle bundle. For muscles with multiple-site damage, an additional 0.5 points were added to the score.

**Preparation of muscle mitochondrial and muscle plasma membrane.** Muscle tissue blocks (0.2-1.0 g) were rinsed in cold normal saline, dried with filter paper and weighed. The blocks were transferred to 10-ml Eppendorf (EP) tubes, cut into small pieces and immediately transferred to a small mortar with ice water. Nine volumes of pre-cooled 0.9% sodium chloride were used to flush residual broken tissue from the EP tubes to obtain a suspension containing 10% muscle tissue homogenate. The samples were ground repeatedly and adequately with a pestle (10-15 min) to prepare a tissue homogenate. The muscle tissue homogenates were transferred to EP tubes, centrifuged at 4°C and 350 x g for 5 min, and the supernatant was collected.

**Mitochondrial preparation.** After centrifugation of the above mentioned 10% tissue homogenate (4°C, 700 x g, 10 min) and sedimentation of cell debris and minor tissue,

the mitochondria were collected via centrifugation at 4°C (3,500 x g for 15 min). The protein concentrations among different samples were standardized by Coomassie staining and spectrophotometry [optical density at 595 nm (OD<sub>595</sub>) was measured].

**Ca<sup>2+</sup>-ATPase detection.** Specific steps were taken according to the kit instructions (ATPase kit; Nanjing Jiancheng Bioengineering Institute, Nanjing, China). One unit of ATPase enzyme activity [ $\mu\text{mol}$  inorganic phosphorus (pi)/mg protein/hour] is defined as the amount of ATPase that catalyzes the production of 1  $\mu\text{mol}$  pi per hour per mg protein. ATPase activity was calculated from the OD using the following formula: ATPase activity =  $[(\text{OD}_{\text{sample}} - \text{OD}_{\text{control}}) / \text{OD}_{\text{standard}}] \times 16.8$ .

**Preparation of RNA samples and complementary (c)DNA by reverse transcription of RNA.** RNA was extracted with TRIzol and the concentration was determined spectrophotometrically. Reverse transcription was performed using the RevertAid First Strand cDNA Synthesis kit (Thermo Fisher Scientific, Inc.). Total RNA (1  $\mu\text{g}$ ), random primers (1  $\mu\text{l}$ ), 5X Reaction Buffer (4  $\mu\text{l}$ ), Ribolock RNase inhibitor (20 U/ $\mu\text{l}$ ; 1  $\mu\text{l}$ ), 10 mM dNTP mix (2  $\mu\text{l}$ ), RevertAid M-MuLv reverse transcriptase (200 U/ $\mu\text{l}$ ; 1  $\mu\text{l}$ ) and nuclease-free water (added to reach a final reaction volume of 20  $\mu\text{l}$ ) were combined into RNase-free tubes on ice. The reaction was gently mixed, centrifuged (350 x g for 1 min at room temperature to avoid blister occurrence) and incubated at 25°C for 5 min, 42°C for 60 min and 70°C for 5 min. The reverse transcription product was used directly for polymerase chain reaction (PCR), stored at -20°C for <1 week, or kept at -70°C for long-term storage.

**PCR amplification.** The following primers were used: GAPDH forward, 5'-GCCGCATCGGTATTCCTTCT-3' and reverse, 5'-GCGTCCAATACGGCCAAATC-3'; interferon (IFN)- $\gamma$  forward, 5'-CACCATCTGGTTGCTGCCTA-3' and reverse, 5'-TACCAGGGTACCAGGCCATT-3'; retinoic acid receptor-related orphan nuclear receptor (ROR) $\gamma$ t forward, 5'-TGATAGGTGGATTTGCGGGA-3' and reverse, 5'-GCTGGGCCAAAGCTAAAGT-3'; and forkhead box (Fox)p3 forward, 5'-TCCACAATGGGACTCATGCC-3' and reverse, 5'-CTGTGGAGAGCTGGTGCATA-3' (all Sangon Biotech, Shanghai, China).

Contents of the PCR mixture were as follows; 12.5  $\mu\text{l}$  2X qPCR Master Mix, 0.5  $\mu\text{l}$  each of forward and reverse primers (0.3  $\mu\text{M}$ ), 1  $\mu\text{l}$  cDNA (500 ng) and nuclease-free water to make the volume up to 25  $\mu\text{l}$ . The contents were mixed and packaged into PCR tubes before being centrifuged for 1 min at 350 x g at room temperature to avoid blister occurrence.

PCR was performed in an iQ5 real-time fluorescent quantitative PCR cyler (Bio-Rad Laboratories, Inc., Hercules, CA, USA). The PCR thermocycling conditions were as follows: Initial denaturation at 95°C for 10 min, annealing at 95°C for 15 sec and denaturation at 60°C for 30 sec for 40 cycles. The extension step was performed at 72°C for 30 sec followed by 80 cycles of final extension at 55-95°C for 30 min to create a dissociation curve. PCR products were quantified using the 2<sup>- $\Delta\Delta\text{Cq}$</sup>  method (29) and GAPDH was used as a reference gene.

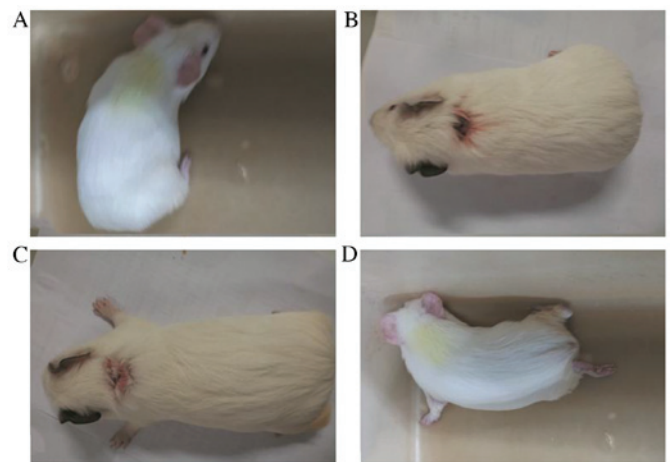


Figure 1. Effects of experimental autoimmune myositis induction. Representative images of guinea pigs immunized with rabbit myosin along with complete Freund's adjuvant and *Mycobacterium tuberculosis*. (A) Pre-immunization: Normal hair color and activity. (B) One week after the second weekly immunization: Depilation and skin ulcers at the dorsal injection site. (C) One week after the third weekly immunization: Humped back while resting, lopped head and flexed forelimb. (D) One week after the fourth weekly immunization: Weakness of limbs and at the last gasp. The images shown are representative of observations in 10 guinea pigs.

**Statistical analysis.** Values are expressed as the mean  $\pm$  standard deviation. Depending on the parameter and comparison, one-way analysis of variance and the least-significant differences test as well as Dunnett's t-tests were performed using SPSS 21.0 statistical software (International Business Machines, Armonk, NY, USA).

## Results

**Clinical manifestations of EAM in guinea pigs treated with NBP.** To establish an animal model of idiopathic inflammatory myopathy, 6- to 8-week-old guinea pigs were obtained and monitored for 7 days. Two out of 40 guinea pigs failed to adapt to their environment, as they ate less and lost weight. However, after another week, nutrition and weight were restored, which suggested successful adaptation to the environment for formal testing.

The guinea pigs were randomly assigned to a normal control group and three EAM model groups (n=10 per group). Guinea pigs in the normal control group showed normal eating and general behavior and had a healthy skin color (Fig. 1A). Guinea pigs in the EAM model group developed redness, swelling and induration (0.4-1.0 cm in diameter) at the injection site after the second week (Fig. 1B). The animals became listless, fearful and thin. The skin started to depilate, the weight gain decreased slightly, movement slowed and the cry of the guinea pigs became low or even hoarse. The symptoms grew progressively more debilitating with time. The body weight ceased to increase or began to decrease in the fourth week, the hair coat became rough and lacklustre, the abdomen and buttocks appeared dirty, signs of malnutrition were apparent, and the guinea pigs developed myasthenia in both forelimbs and were unable to hold up their extremities (Fig. 1C). One guinea pig had severe myasthenia and lay laterally (Fig. 1D). The animal was immediately



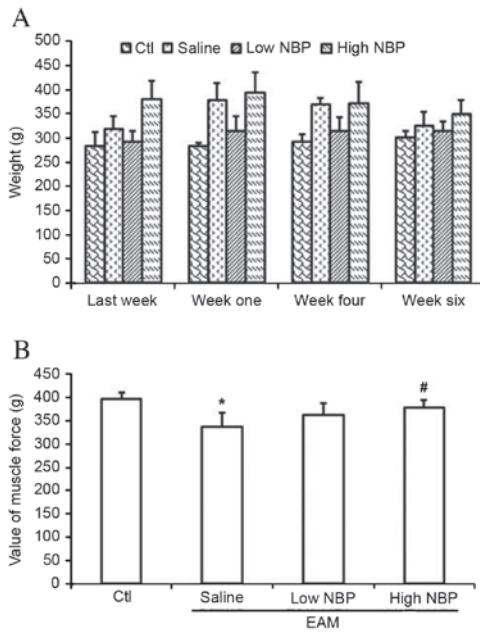


Figure 2. Effects of NBP on muscle weight and strength of guinea pigs with EAM. (A) Weight of groups of guinea pigs over time. 'Last week' represents one week prior to immunization. 'Week one' and 'week four' represent one week after the first and the fourth immunization, respectively. 'Week six' represents one week after animals had been administered NBP in the fifth week. (B) Myodynamia measurements in the different groups. Values are expressed as the mean  $\pm$  standard deviation (n=10 per group). Groups: Ctl, normal control group; saline, normal saline EAM group; low NBP, low-dose (40  $\mu$ l/40 mg/kg wt NBP) EAM group; high-NBP, high-dose (80  $\mu$ l/80 mg/kg wt NBP) EAM group. \*P<0.05 vs. Ctl; #P<0.05 vs. saline group. EAM, experimental autoimmune myositis; NBP, 3-n-butylphthalide; Ctl, control.

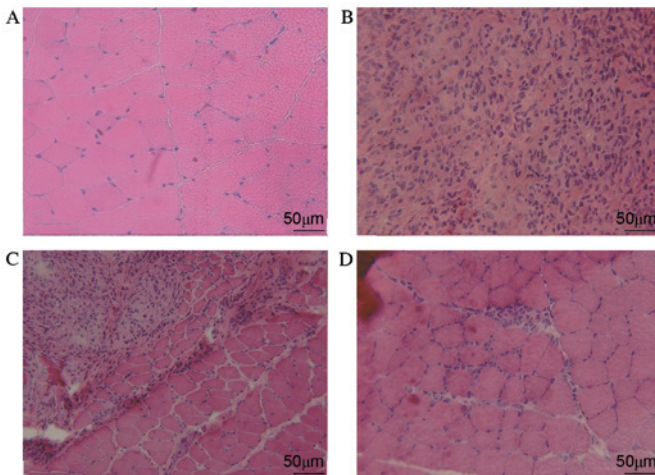


Figure 3. Histopathological effects of NBP on muscle structure in guinea pigs with EAM. Histopathological staining of muscle tissues from (A) control guinea pigs without EAM induction; (B) EAM guinea pigs treated with normal saline; (C) EAM guinea pigs treated with low-dose (40  $\mu$ l/40 mg/kg wt) NBP; and (D) EAM guinea pigs treated with high-dose (80  $\mu$ l/80 mg/kg wt) NBP (magnification,  $\times$ 200; scale bar, 50  $\mu$ m; hematoxylin and eosin staining). Images are representative of 8 sections per guinea pig (n=10). EAM, experimental autoimmune myositis; NBP, 3-n-butylphthalide.

ethanised by exsanguination under anesthesia (intraperitoneal injection of 15 mg/kg sodium pentobarbital; Sigma-Aldrich; Merck KGaA). Simultaneously, blood samples and muscle specimens were collected.

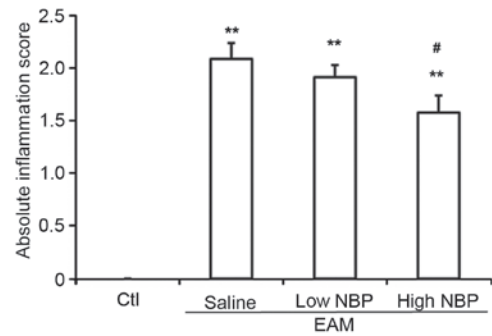


Figure 4. Absolute inflammation scores in EAM guinea pigs upon NBP treatment. Staining values were calculated for 8 sections (4 fields each) for control guinea pigs without EAM induction, and EAM guinea pigs treated with normal saline, low-dose (40  $\mu$ l/40 mg/kg wt) NBP or high-dose (80  $\mu$ l/80 mg/kg wt) NBP group. Values are expressed as the mean  $\pm$  standard deviation (n=10 per group). \*\*P<0.01 vs. control group; #P<0.05 vs. saline group. EAM, experimental autoimmune myositis; NBP, 3-n-butylphthalide; Ctl, control.

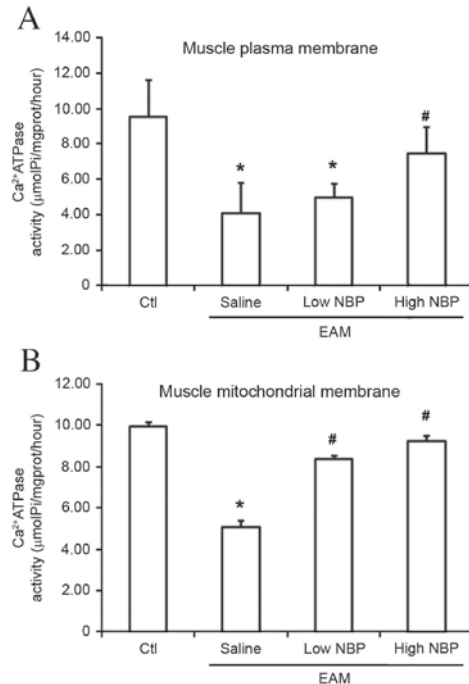


Figure 5. Effects of NBP on Ca<sup>2+</sup>-ATPase concentrations in the muscle mitochondrial and muscle plasma membranes of EAM guinea pigs. Ca<sup>2+</sup>-ATPase concentrations (A) in the muscle plasma membrane and (B) in the mitochondrial membrane were determined in skeletal muscle tissue of guinea pigs from control guinea pigs without EAM induction, and EAM guinea pigs treated with normal saline, low-dose (40  $\mu$ l/40 mg/kg wt) NBP or high-dose (80  $\mu$ l/80 mg/kg wt) NBP group (n=10). Values are expressed as the mean  $\pm$  standard deviation (n=10 per group). \*P<0.05 vs. control group; #P<0.05 vs. saline group. EAM, experimental autoimmune myositis; NBP, 3-n-butylphthalide; Ctl, control.

To determine the effects of NBP on guinea pigs with EAM, the animals with induced EAM were treated with normal saline and low- or high-dose NBP (n=10 guinea pigs per group). In guinea pigs with EAM treated with low-dose NBP, the weight was not obviously affected. The EAM/high-dose NBP group had more weight gain than the normal saline group, but the differences were not significant (Fig. 2A). However, the guinea pigs in the EAM/normal saline group had significantly lower strength than those in the control group (P=0.036; Fig. 2B).

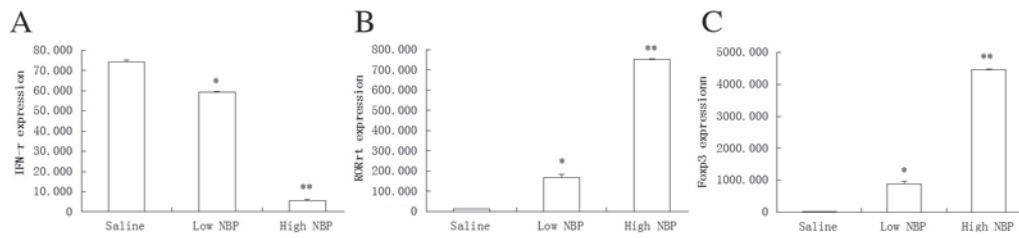


Figure 6. Effects of NBP on the mRNA expression levels of IFN- $\gamma$ , ROR $\gamma$ t and Foxp3 in muscle tissue of EAM guinea pigs. The relative mRNA (house-keeping gene GAPDH) expression of (A) IFN- $\gamma$ , (B) ROR $\gamma$ t and (C) Foxp3 were determined in skeletal muscle tissue samples from EAM guinea pigs. Saline represents the EAM/saline vehicle injection group, low NBP represents the low-dose (40  $\mu$ l/40 mg/kg wt) NBP group, and high NBP represents the high-dose (80  $\mu$ l/80 mg/kg wt) NBP group. Values are expressed as the mean  $\pm$  standard deviation (n=10 per group). \*P<0.05, \*\*P<0.01 vs. saline group. EAM, experimental autoimmune myositis; NBP, 3-n-butylphthalide; IFN- $\gamma$ , interferon- $\gamma$ ; ROR $\gamma$ t, retinoic acid receptor-related orphan nuclear receptor  $\gamma$ t; Foxp3, forkhead box p3.

The guinea pigs with EAM treated with MBP had a higher strength than those in the EAM/normal saline group, with the difference being significant in the EAM/high dose NBP group (P=0.045). These results suggested that NBP partially reversed the myasthenia caused by EAM.

*Histopathological changes in the muscles of NBP-treated EAM guinea pigs.* To determine the effects of NBP at the microscopic level, muscle tissues were subjected to histopathological analysis. The degree of inflammatory cell infiltration was low in control guinea pigs (Fig. 3A), but was clearly increased upon EAM induction (Fig. 3B). EAM guinea pigs treated with low-dose NBP (Fig. 3C) showed a slight reduction in the inflammatory cell infiltration, while EAM guinea pigs treated with high-dose NBP (Fig. 3D) showed a marked reduction in inflammatory cell infiltration. The levels of inflammation in the 4 groups of guinea pigs were scored by selecting 4 visual fields in each of the 8 sections per guinea pig (n=10 guinea pigs per group). Compared with the normal control group, the EAM group had a significantly increased pathological inflammation score (P<0.01). Compared with the EAM/normal saline group, the EAM/high dosage NBP group had a significantly reduced pathological inflammation score (P<0.05). The EAM/low dose-NBP group also showed a reduction, which was not significant (Fig. 4).

*Effect of NBP on Ca<sup>2+</sup>-ATPase activity.* To verify the above-mentioned findings at the molecular level, the Ca<sup>2+</sup>-ATPase activity of the muscle mitochondrial membrane and muscle plasma membrane was measured. Each of these measures of muscle activity was significantly decreased upon EAM induction. However, this decrease was significantly attenuated in the EAM/high-dose NBP group compared with the EAM/normal saline group (P<0.05; Fig. 5), confirming that NBP reverses the effects of EAM on muscle activity. In the EAM/low-dose NBP group, Ca<sup>2+</sup>-ATPase activity in the muscle mitochondrial membrane was also significantly increased compared with the EAM/saline group (P<0.05; Fig. 5).

*Effect of NBP on mRNA expression of IFN- $\gamma$ , ROR $\gamma$ t, and Foxp3 in muscle tissue.* To determine the effects of NBP on T-cell-associated cytokines, the mRNA expression levels of IFN- $\gamma$ , ROR $\gamma$ t and Foxp3 in muscle tissues were measured. The expression of IFN- $\gamma$  mRNA was significantly reduced by NBP (P<0.01; Fig. 6A), whereas Foxp3 and ROR $\gamma$ t mRNA

expression levels were significantly elevated by NBP (P<0.01; Fig. 6B and C).

## Discussion

Rats and guinea pigs have been previously used to study EAM (30-33). Since rabbit and guinea pig skeletal muscle myosin proteins cross-react with each other, emulsified purified rabbit skeletal muscle tissue homogenate and adjuvant were subcutaneously injected to immunize guinea pigs to establish the EAM model.

After the guinea pigs were introduced to the new environment, their weights appeared to decrease, probably due to poor adaptation, and failed to return to normal until day 7. Only those animals that returned to normal weight were used in the present experiments. Similar to the results of other studies, slight weight loss occurred during immune injection, but without any significant difference between the vehicle injection group and myosin injection group (34,35). Ito *et al* (28) immunized Lewis rats with purified rabbit skeletal myosin, and the weight of the EAM and the control group increased. Four weeks after immunization, the body weight in the EAM group was significantly lower than that in the control group. In the present study, there was no difference in the weight of the four groups of guinea pigs prior to myosin immunization, weeks 1 and 4 of immunization, and after injection of low-dose and high-dose NBP.

When Nemoto *et al* (34) and Kojima *et al* (27) immunized Lewis rats with purified rabbit skeletal myosin, a slight weakness appeared, but there was no significant difference between the adjuvant control group and the EAM group. Nakano *et al* (35) immunized Wistar rats with laminin and obtained the same results. Ito *et al* (28) immunized Lewis rats with purified rabbit skeletal myosin: The EAM group moved less than the control group but did not appear to have myasthenia. However, EAM myodynamic evaluation was performed using the myasthenia classification method of Matsubara and Takamori (36), which failed to detect slight differences. EAM myodynamia was also evaluated through an inverted mesh, and rat myodynamia was significantly reduced (14). In the present study, a dynamometer was used instead of the myasthenia classification method and inverted mesh, which is more sensitive and accurate. Myodynamia in the EAM/normal saline group was found to be significantly lower than that in the normal control group in the present study.

NBP has been reported to reduce cerebral infarction and neurologic impairment induced by diabetes (10). Taken orally, 30 mg/kg NBP only mildly improved the athletic ability of Tg (SOD1-G93A) transgenic rats (amyotrophic lateral sclerosis (ALS) animal model), but 60 mg/kg NBP significantly slowed the athletic ability in the ALS model (11). The present study demonstrated that loss of myodynamia in the EAM/normal saline group was restored in the EAM/high-dose NBP group, indicating that high-dose NBP restores the myodynamia of EAM animals.

Idiopathic inflammatory myopathies (myositis for short) include dermatomyositis, PM, necrotizing myopathy and inclusion body myositis. Each type differs in the pathogenesis and clinical manifestation, but muscle biopsies are necessary for reliable diagnosis to distinguish PM from other types of myopathy. Clinically and pathologically, EAM is reflective of human PM, but PM is an extremely complex disease with varying pathology (6). In the present study, in the EAM/normal saline group, myodynamia was reduced but the inflammatory score was significantly higher than that in the control group, which indicates that the EAM model was successfully established.

NBP significantly reduces the cerebral infarction area (37): 20 mg/kg NBP reduces the classic neuropathological changes in the hippocampus of rats with chronic cerebral ischemia, including neuronal loss, nuclear shrinkage and cerebral edema (38). A combination of 30 mg/kg NBP and 20 mg/kg amantadine obviously reduced the neurodegenerative pathology of the CA1 hippocampus and parietal cortex in aging rats, including neuronal loss and neuron shrinkage (39). NBP reduces granulocyte infiltration at the brain injury-associated infarcted sites after ischemia and effectively protects against inflammation at ischemia sites (12). Consistently, in the present study, the inflammation in the NBP group was milder than that in the normal saline group.

Cell membrane ATPases maintain the resting membrane potential and regulate the intracellular and extracellular balance of calcium ions (40). In the muscle cell membrane and mitochondrial membrane,  $\text{Ca}^{2+}$ -ATPase activity requires a concentration gradient across the membrane for cellular excitability. Intracellular  $\text{K}^{+}$  loss and extracellular  $\text{Na}^{+}$  inflow result in an increased muscle cell membrane depolarization threshold and decline in muscle capacity. Normal sodium calcium levels are reversed, which further increases the intracellular  $\text{Ca}^{2+}$  overload, activates proteolytic enzymes and promotes cell death (41). In the present study, intraperitoneal injection of high-dose NBP (80 mg/kg) led to a significant increase in  $\text{Ca}^{2+}$ -ATPase activity in the guinea pig EAM model, which suggests that NBP protects the EAM mitochondria and the muscle plasma membrane. In the low-dose NBP group, no significant increase was observed in  $\text{Ca}^{2+}$ -ATPase activity in the muscle plasma membrane, whereas activity was significantly increased in the muscle mitochondrial membrane.

NBP also modulated the expression of selected T-cell-associated cytokines.  $\text{IFN-}\gamma$  is the main cytokine produced by Type 1 T-helper (Th1) cells, which mediate cellular immune responses to induce inflammation.  $\text{ROR}\gamma\text{t}$  is an important transcription factor that polarizes the differentiation of Th cells into Th1 cells (42).

T-regulatory (Treg) cells have immune suppressor functions, and  $\text{Foxp3}$ , a member of the forkhead transcription factor family, is considered as a marker of Treg cells.  $\text{Foxp3}$  regulates Treg cell activity via direct regulation of multiple genes. The increase of autoimmunity and tissue inflammation by Tr1 cells occurs via secretion of immunosuppressive cytokines, but the expression of  $\text{Foxp3}$  is lacking (43).  $\text{Foxp3}(+)$  Tregs are known to function as major regulators of immune homeostasis through their immunosuppressive function (44). The Th17 lineage is a  $\text{CD4}(+)$  T cell subset that exerts its function by secreting proinflammatory cytokines and protecting the host against microbial infections (45). The altered ratio of  $\text{Foxp3}(+)$  Tregs to Th17 cells serves an important role in the pathogenesis of immune-related diseases (46). In the present study, the mRNA expression of  $\text{IFN-}\gamma$  was significantly reduced, whereas the expressions of  $\text{Foxp3}$  and  $\text{ROR}\gamma\text{t}$  were significantly increased by NBP compared with the EAM/saline group. The effect of NBP on  $\text{IFN-}\gamma$  and  $\text{ROR}\gamma\text{t}/\text{Foxp3}$  expression suggests that NBP may inhibit Th1 differentiation and/or function and provoke Th17/Treg differentiation and/or function in the pathogenesis of EAM. It may be speculated that NBP has therapeutic effects on EAM that are attributable, at least in part, to enhanced Th17/Treg function.

In conclusion, the guinea pig model of EAM was successfully established in the present study. It was demonstrated that high-dose NBP significantly improved the myodynamia of EAM animals and reduced the pathology regarding inflammatory cell infiltration. NBP also improved the  $\text{Ca}^{2+}$ -ATPase activity of the EAM muscle mitochondrial and muscle plasma membrane. NBP reduced the  $\text{IFN-}\gamma$  transcription in muscle cells and significantly increased the mRNA expression of  $\text{ROR}\gamma\text{t}/\text{Foxp3}$ . These results provided a basis for further studies to determine the intervention strategies using NBP.

## Acknowledgements

This work was supported by the National Natural Science Foundation of China (grant no. 81271399) and the National Science Foundation of Beijing (grant no. 7132216).

## References

- Vincze M and Danko K: Idiopathic inflammatory myopathies. *Best Pract Res Clin Rheumatol* 26: 25-45, 2012.
- Dimachkie MM and Barohn RJ: Idiopathic inflammatory myopathies. *Semin Neurol* 32: 227-236, 2012.
- Cox S, Limaye V, Hill C, Blumbergs P and Roberts-Thomson P: Idiopathic inflammatory myopathies: Diagnostic criteria, classification and epidemiological features. *Int J Rheum Dis* 13: 117-124, 2010.
- Szodoray P, Alex P, Knowlton N, Centola M, Dozmorov I, Csipo I, Nagy AT, Constantin T, Ponyi A, Nakken B and Danko K: Idiopathic inflammatory myopathies, signified by distinctive peripheral cytokines, chemokines and the TNF family members B-cell activating factor and a proliferation inducing ligand. *Rheumatology (Oxford)* 49: 1867-1877, 2010.
- Gazeley DJ and Cronin ME: Diagnosis and treatment of the idiopathic inflammatory myopathies. *Ther Adv Musculoskelet Dis* 3: 315-324, 2011.
- Carstens PO and Schmidt J: Diagnosis, pathogenesis and treatment of myositis: Recent advances. *Clin Exp Immunol* 175: 349-358, 2014.
- Bodoki L, Vincze M, Griger Z and Dankó K: Intravenous immunoglobulin treatment in idiopathic inflammatory myopathy. *Orv Hetil* 154: 723-728, 2013 (In Hungarian).



8. Mathur T, Manadan AM, Thiagarajan S, Hota B and Block JA: Corticosteroid monotherapy is usually insufficient treatment for idiopathic inflammatory myopathy. *Am J Ther* 22: 350-354, 2015.
9. Wilson CW III: Relative recovery and identification of carbonyl compounds from celery essential oil. *J Food Sci* 35: 766-768, 1970.
10. Zhang T, Yan W, Li Q, Fu J, Liu K, Jia W, Sun X and Liu X: 3-n-Butylphthalide (NBP) attenuated neuronal autophagy and amyloid- $\beta$  expression in diabetic mice subjected to brain ischemia. *Nerol Res* 33: 396-404, 2011.
11. Feng X, Peng Y, Liu M and Cui L: DL-3-n-butylphthalide extends survival by attenuating glial activation in a mouse model of amyotrophic lateral sclerosis. *Neuropharmacology* 62: 1004-1010, 2012.
12. Xu HL and Feng YP: Inhibitory effects of chiral 3-n-butylphthalide on inflammation following focal ischemic brain injury in rats. *Acta Pharmacol Sin* 21: 433-438, 2000.
13. Wang HM, Zhang T, Huang JK and Sun XJ: 3-N-butylphthalide (NBP) attenuates the amyloid- $\beta$ -induced inflammatory responses in cultured astrocytes via the nuclear factor- $\kappa$ B signaling pathway. *Cell Physiol Biochem* 32: 235-242, 2013.
14. Allenbach Y, Solly S, Grégoire S, Dubourg O, Salomon B, Butler-Browne G, Musset L, Herson S, Klatzmann D and Benveniste O: Role of regulatory T cells in a new mouse model of experimental autoimmune myositis. *Am J Pathol* 174: 989-998, 2009.
15. Wang YG, Li Y, Wang CY, Ai JW, Dong XY, Huang HY, Feng ZY, Pan YM, Lin Y, Wang BX and Yao LL: L-3-n-Butylphthalide protects rats' cardiomyocytes from ischaemia/reperfusion-induced apoptosis by affecting the mitochondrial apoptosis pathway. *Acta Physiol (Oxf)* 210: 524-533, 2014.
16. Xin DL, Harris MY, Wade CK, Amin M, Barr AE and Barbe MF: Aging enhances serum cytokine response but not task-induced grip strength declines in a rat model of work-related musculoskeletal disorders. *BMC Musculoskelet Disord* 12: 63, 2011.
17. Mitzelfelt JD, Dupree JP, Seo DO, Carter CS and Morgan D: Effects of chronic fentanyl administration on physical performance of aged rats. *Exp Gerontol* 46: 65-72, 2011.
18. Kietrys DM, Barr AE and Barbe MF: Exposure to repetitive tasks induces motor changes related to skill acquisition and inflammation in rats. *J Mot Behav* 43: 465-476, 2011.
19. Michael G, Kane KA and Coker SJ: Adrenaline reveals the torsadogenic effect of combined blockade of potassium channels in anaesthetized guinea pigs. *Br J Pharmacol* 154: 1414-1426, 2008.
20. Mengistu M, Abebe Y, Mekonnen Y and Tolessa T: *In vivo* and *in vitro* hypotensive effect of aqueous extract of *Moringa stenopetala*. *Afr Health Sci* 12: 545-551, 2012.
21. Johnson DM, Geys R, Lissens J and Guns PJ: Drug-induced effects on cardiovascular function in pentobarbital anesthetized guinea-pigs: Invasive LVP measurements versus the QA interval. *J Pharmacol Toxicological Methods* 66: 152-159, 2012.
22. Guns PJ, Johnson DM, Weltens E and Lissens J: Negative electro-mechanical windows are required for drug-induced Torsades de Pointes in the anesthetized guinea pig. *J Pharmacol Toxicol Methods* 66: 125-134, 2012.
23. Mooney L, Marks L, Philp KL, Skinner M, Coker SJ and Currie S: Optimising conditions for studying the acute effects of drugs on indices of cardiac contractility and on haemodynamics in anaesthetized guinea pigs. *J Pharmacol Toxicol Methods* 66: 43-51, 2012.
24. Kågström J, Laumola EL, Poijes N, Johansson M and Ericson AC: Assessment of the effects of changes in body temperature on cardiac electrophysiology in anaesthetised guinea pigs. *J Pharmacol Toxicol Methods* 65: 1-7, 2012.
25. Michael G, Kane KA and Coker SJ: Adrenaline reveals the torsadogenic effect of combined blockade of potassium channels in anaesthetized guinea pigs. *Br J Pharmacol* 154: 1414-1426, 2008.
26. Lopes FDTQS, Alvarenga GS, Quiles R, Dorna MB, Vieira JE, Dolnikoff M and Martins MA: Pulmonary responses to tracheal or esophageal acidification in guinea pigs with airway inflammation. *J Appl Physiol* 93: 842-847, 2002.
27. Kojima T, Tanuma N, Aikawa Y, Shin T, Sasaki A and Matsumoto Y: Myosin-induced autoimmune polymyositis in the rat. *J Neurol Sci* 151: 141-148, 1997.
28. Ito T, Kumamoto T, Horinouchi H, Yukishige K, Sugihara R, Fujimoto S and Tsuda T: Adhesion molecule expression in experimental myositis. *Muscle Nerve* 25: 409-418, 2002.
29. Livak KJ and Schmittgen TD: Analysis of relative gene expression data using real-time quantitative PCR and the 2(-Delta Delta C(T)) method. *Methods* 25: 402-408, 2001.
30. Currie S: Experimental myositis: The in-vivo and in-vitro activity of lymph-node cells. *J Pathol* 105: 169-185, 1971.
31. Dawkins RL: Experimental myositis associated with hypersensitivity to muscle. *J Pathol Bacteriol* 90: 619-625, 1965.
32. Kalden JR, Williamson WG and Irvine WJ: Experimental myasthenia gravis, myositis and myocarditis in guinea-pigs immunized with subcellular fractions of calf thymus or calf skeletal muscle in Freund's complete adjuvant. *Clin Exp Immunol* 13: 79-88, 1973.
33. Wen-Jing L, Chuan-Qiang P, Hong-Hua L, Xiang-Hui L and Jie-Xiao L: A new modified animal model of myosin-induced experimental autoimmune myositis enhanced by defibrase. *Arch Med Sci* 11: 1272-1278, 2015.
34. Nemoto H, Bhopale MK, Constantinescu CS, Schotland D and Rostami A: Skeletal muscle myosin is the autoantigen for experimental autoimmune myositis. *Exp Mol Pathol* 74: 238-243, 2003.
35. Nakano J, Yoshimura T, Okita M, Motomura M, Kamei S, Matsuo H and Eguchi K: Laminin-induced autoimmune myositis in rats. *J Neuropathol Exp Neurol* 64: 790-796, 2005.
36. Matsubara S and Takamori M: Experimental allergic myositis: Strain 13 guinea pig immunised with rabbit myosin B fraction. *Acta Neuropathol* 74: 158-162, 1987.
37. Zhao Q, Zhang C, Wang X, Chen L, Ji H and Zhang Y: (S)-ZJM-289, a nitric oxide-releasing derivative of 3-n-butylphthalide, protects against ischemic neuronal injury by attenuating mitochondrial dysfunction and associated cell death. *Neurochem Int* 60: 134-144, 2012.
38. Xu J, Wang Y, Li N, Xu L, Yang H and Yang Z: L-3-n-butylphthalide improves cognitive deficits in rats with chronic cerebral ischemia. *Neuropharmacology* 62: 2424-2429, 2012.
39. Ma S, Xu S, Liu B, Li J, Feng N, Wang L and Wang X: Long-term treatment of l-3-n-butylphthalide attenuated neurodegenerative changes in aged rats. *Naunyn Schmiedebergs Arch Pharmacol* 379: 565-574, 2009.
40. Cartwright EJ, Oceandy D, Austin C and Neyses L: Ca<sup>2+</sup> signaling in cardiovascular disease: The role of the plasma membrane calcium pumps. *Sci China Life Sci* 54: 691-698, 2011.
41. Despa S and Bers DM: Na<sup>+</sup> transport in the normal and failing heart-remember the balance. *J Mol Cell Cardiol* 61: 2-10, 2013.
42. Tajiri K, Shimojo N, Sakai S, Machino-Ohtsuka T, Imanaka-Yoshida K, Hiroe M, Tsujimura Y, Kimura T, Sato A, Yasutomi Y and Aonuma K: Pitavastatin regulates helper T-cell differentiation and ameliorates autoimmune myocarditis in mice. *Cardiovasc Drugs Ther* 27: 413-424, 2013.
43. Pot C, Apetoh L and Kuchroo VK: Type 1 regulatory T cells (Tr1) in autoimmunity. *Semin Immunol* 23: 202-208, 2011.
44. Carvalho MI, Pires I, Prada J, Gregório H, Lobo L and Queiroga FL: Intratumoral FoxP3 expression is associated with angiogenesis and prognosis in malignant canine mammary tumors. *Vet Immunol Immunopathol* 178: 1-9, 2016.
45. Pasztoi M, Bonifacius A, Pezoldt J, Kulkarni D, Niemz J, Yang J, Teich R, Hajek J, Pisano F, Rohde M, *et al*: Yersinia pseudo-tuberculosis supports Th17 differentiation and limits de novo regulatory T cell induction by directly interfering with T cell receptor signaling. *Cell Mol Life Sci* 74: 2839-2850, 2017.
46. Du R, Zhao H, Yan F and Li H: IL-17+Foxp3+ T cells: An intermediate differentiation stage between Th17 cells and regulatory T cells. *J Leukoc Biol* 96: 39-48, 2014.



This work is licensed under a Creative Commons Attribution-NonCommercial-NoDerivatives 4.0 International (CC BY-NC-ND 4.0) License.